Journal of Alloys and Compounds 521 (2012) 66–70

Contents lists available at SciVerse ScienceDirect

Journal of Alloys and Compounds

journal homepage: www.elsevier.com/locate/jallcom

# Platinum boride nanowires: Synthesis and characterization

Zhan-Hui Ding[a,b], Li-Xia Qiu[a], Jian Zhang[c], Bin Yao[c], Tian Cui[c], Wei-Ming Guan[d], Wei-Tao Zheng[e], Wen-Quan Wang[a], Xu-Dong Zhao[b], Xiao-Yang Liu[b,*]

[a] College of Physics, Jilin University, Changchun 130012, China
[b] Key Lab of Inorganic Synthesis and Preparative Chemistry, Jilin University, Changchun 130012, China
[c] Key Lab of Superhard Materials, Jilin University, Changchun 130012, China
[d] Kunming Institute of Precious Metals, Kunming, 650106, China
[e] College of Material Science and Engineering, Jilin University, Changchun 130012, China

ARTICLE INFO

*Article history:*
Received 25 November 2011
Received in revised form 3 January 2012
Accepted 5 January 2012
Available online 14 January 2012

*Keywords:*
Platinum boride
Nanowires
DC arc
VLS

ABSTRACT

Platinum boride (PtB) nanowires have been successfully fabricated with direct current arc discharge method using a milled mixture of platinum (Pt) and boron nitride (BN) powders. X-ray diffraction (XRD), scanning electron microscopy (SEM) and transmission electron microscopy (TEM) were used to characterize the compositions, morphology, and structures of the samples. The results show that PtB nanowires are 30–50 nm thick and 20–30 μm long. TEM and selected area electron diffraction (SAED) patterns identify that the PtB nanowires are single-crystalline in nature. A growth mechanism based on vapor–liquid–solid (VLS) process is proposed for the formation of nanowires.

© 2012 Elsevier B.V. All rights reserved.

## 1. Introduction

Transition metal (TM) borides are attracting increasing interest due to their importance in both fundamental science and technological applications. Many TM borides have found applications as abrasives or "ultra high-temperature ceramics" [1–4]. Recently, the borides of noble metal Os [5], Re [6], Ru [7], Rh and Ir [8] have been synthesized under extreme conditions. All of these noble metals borides have high bulk modulus and were described as superhard materials [9]. As for platinum (Pt), although the structures of platinum borides (PtB) have been known since 1960, when Aronsson et al. [10] described PtB crystallized in anti-NiAs structure, only limited data about PtB are available in the literatures up-to-date, the mechanical, optical and electrical properties of this material are still unknown. The lack of detailed information on the physical properties results in the restricted potential application of this compound.

One-dimension (1D) nanostructures, such as nanotubes, nanowires and nanobelts have attracted much attention because of their novel properties and potential applications [11,12]. For example, $Al_4B_2O_9$ and $Al_{18}B_4O_{33}$ nanowires [13] have been synthesized by combustion method, $SrB_2O_4$ nanorods [14] have been synthesized *via* sol–gel route, $Ca_2B_2O_5$ nanobelts and nanogrooves [15] have been synthesized through hydrothermal technique, $CaB_6$ [16] and$CeB_6$ [17] nanowires have been synthesized by CVD method. In this paper, we report the synthesis PtB nanowires by the direct current arc discharge technique. To our knowledge, this is the first report on synthesis of 1D PtB nanostructures. PtB nanowires have potential use in nanocomposites, where they may impart stiffness, toughness, and strength of the materials. They are also promising materials used in nanoelectronic devices, especially in high temperature nanoelectronic devices. The mechanism of growth of PtB nanowires is discussed in the present work.

## 2. Experimental

The starting materials were platinum (Pt) powders (Cuibolin, Beijing, purity 99.9%) with a particle size smaller than 130 μm and *h*-BN powders (Alfa Aesar, purity 99.95%) with a particle size smaller than 100 μm, respectively. The Pt and *h*-BN powders were mixed in a molar ratio of 1:20, in order to compensate the evaporative loss of boron atoms during the synthesis. Then the mixtures were mechanically milled under Ar ambient in a P-7 planetary mill (Fritsch, Germany) using hardened bearing-steel balls (5 and 10 mm in diameter). The rotational speed of the hardened steel vials was 600 rpm while the ball-to-powder weight ratio $C_{bp}$ was 10. The total milling time is 40 h.

The direct current (DC) arc discharge system is shown schematically in Fig. 1. A tungsten rod (purity: 99.99%, 8 mm in diameter and 30 cm in length) was used as the cathode. The 40 h milled powders pressed into columns (10 mm in diameter and 3 mm in height) are used as the reactants and placed in the water-cooled graphite crucible which acted as the anode. The reaction chamber was flushed firstly for several times by firstly evacuating the chamber to less than 1 Pa and then filled with argon to remove the residual air, and then was filled with the Ar gas of 10 kPa as

* Corresponding author at: College of Chemistry, Jilin University, 2699 Qianjin Street, Changchun, 130012, China. Tel.: +86 431 85168316.
*E-mail address:* Liuxy@jlu.edu.cn (X.-Y. Liu).

0925-8388/$ – see front matter © 2012 Elsevier B.V. All rights reserved.
doi:10.1016/j.jallcom.2012.01.038

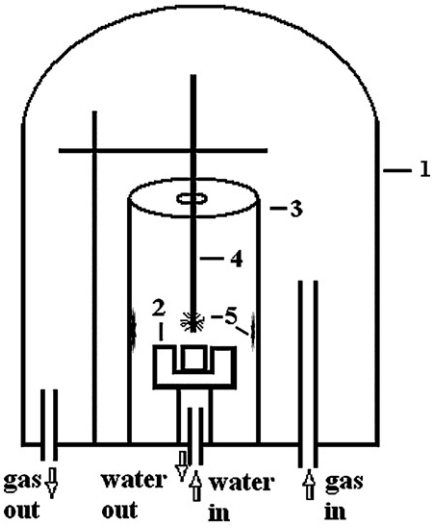


**Fig. 1.** A sketch map of the direct current arc discharge system. (1) The reaction chamber. (2) The water-cooled crucible (anode). (3) The water-cooled collecting wall. (4) The tungsten rod (cathode). (5) The sample-collecting regions.

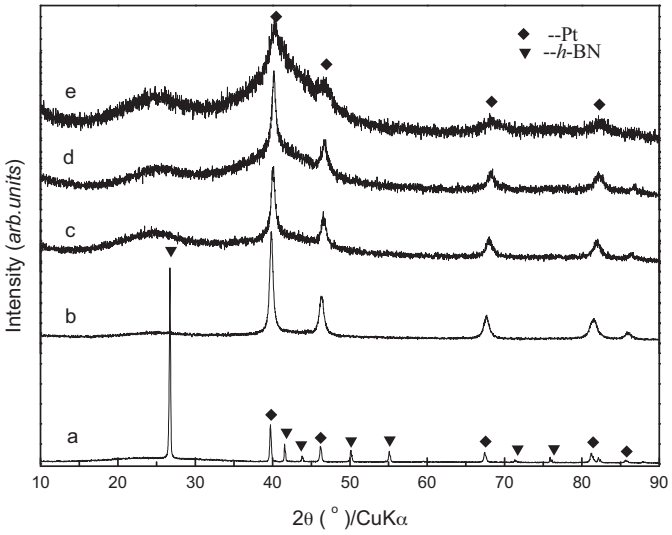


**Fig. 2.** XRD patterns for the platinum and boron nitride powder mixture milling. (a) 0 h; (b) 10 h; (c) 20 h; (d) 30 h; and (e) 40 h.

working gas. As the direct current arc discharge was ignited, the input current was maintained at 100 A and the voltage was a little higher than 20 V. The power supply was turned off 10 min later. After being passivated in Ar for 6 h, the sample was gathered at the water-cooled collecting wall (see Fig. 1).

The structural analysis of products was carried out by X-ray diffraction (Cu $K_\alpha$ radiation, Rigaku D/max 2550VB, Japan). The SEM images of the sample were taken on a scanning electron microscopy (JSM-6700F, JEOL). The morphology of the nanowires, as well as the selected area electron diffraction (SAED) pattern, was obtained *via* an H-8100 microscope using an accelerating voltage of 200 kV. The TEM micrographs of representative nanowires were obtained on a JEOL JEM-2000EX microscope. The photoluminescence (PL) spectra were recorded at room temperature by a Renishaw invia spectrometer with the excitation wavelength of 532 nm.

## 3. Results and discussions

Mechanical milling is an effective technique for producing metallic powders in the solid state [18]. Powder particles in the ball mill are subjected to high-energy collision which causes the powder particles to be cold welded together and fracture. Cold welding and fracturing enable powder particles to be always in contact with each other and atomically clean surfaces and with minimized diffusion distance. Therefore, mechanical milling can greatly decrease the activation energy and increase the reaction rate of the reactants. Using this technique, refractory materials such as TiN [19], ZrN [20] and HfN [21] have been successfully prepared. In the present work, mechanical milling was used for producing platinum nanoparticals and amorphous BN (*a*-BN) powders, which are benefit for Pt react with B atoms of *a*-BN to form PtB in the DC arc discharge system.

The XRD patterns of the mixture of Pt and *h*-BN powders milled for different time periods are shown in Fig. 2. After milling of 10 h (Fig. 2(b)), all diffraction peaks of *h*-BN disappear, at the same time, a broad peak is observed at about $2\theta = 20^\circ$, indicating the complete transformation of *h*-BN into *a*-BN. With the milling time increasing, the intensities of Pt diffraction peaks decrease while the corresponding the full width at half-maximum (FWHM) increased, as shown in Fig. 2. The grain sizes of Pt was calculated by Scherrer formula ($D = 0.89\lambda/B\cos\theta$, where $\lambda$ is the X-ray wavelength, $B$ is FWHM and $\theta$ is Bragg diffraction angle), the results are summarized in Fig. 3. It is shown that the grain size of Pt in the raw mixtures is about 42 nm, and decreases to 5 nm after milling for 40 h. In addition, the lattice constant of Pt obtained at various milling times have also been calculated, as shown in Fig. 3, indicating that the lattice

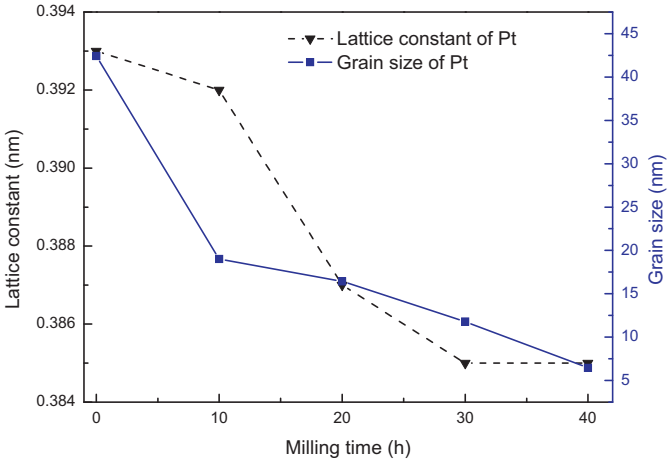


**Fig. 3.** Dependences of crystallite size and lattice constant of platinum on milling time.

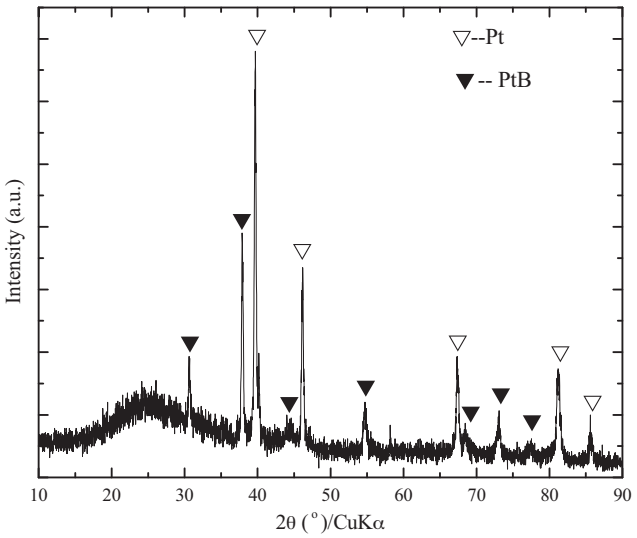


**Fig. 4.** The XRD patterns for the samples collected in the DC arc discharge system.

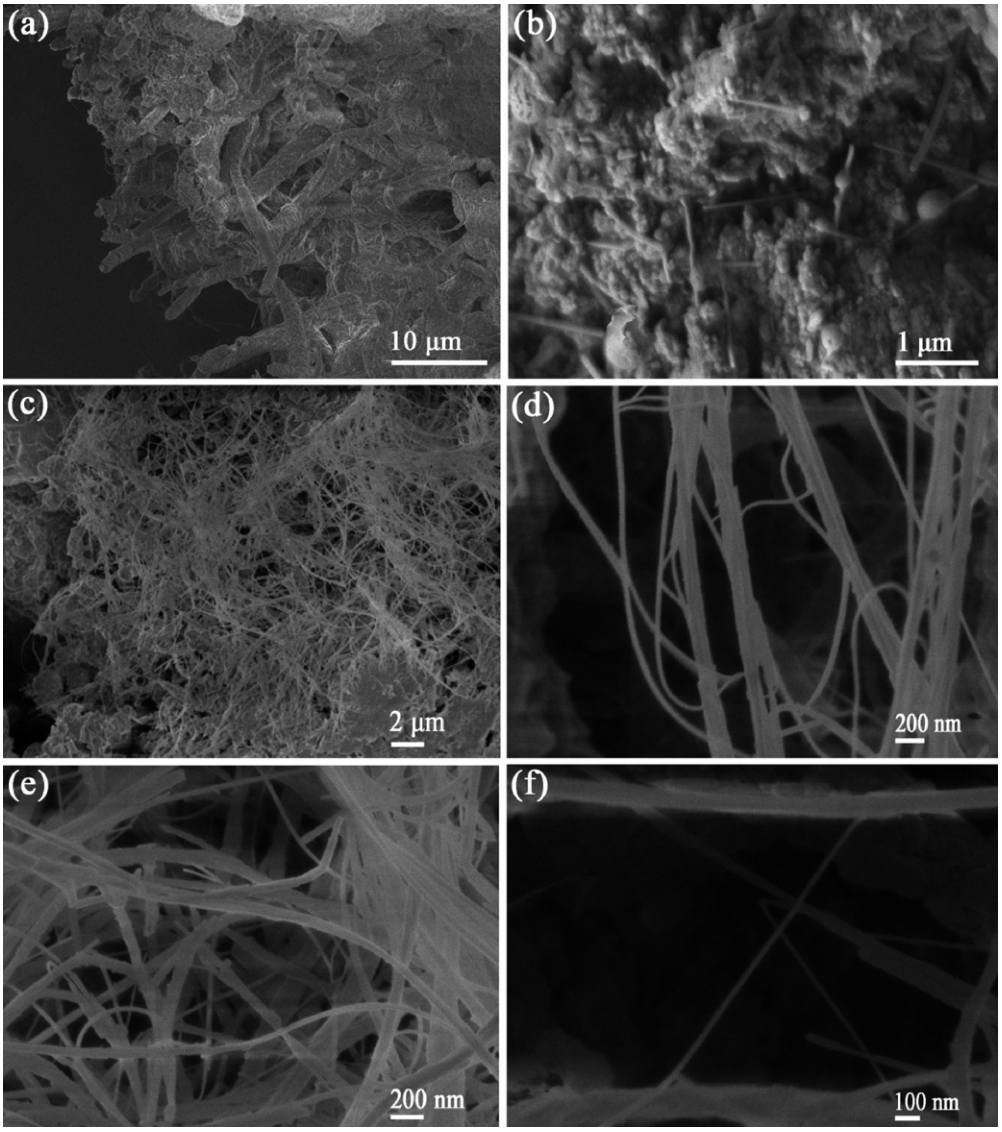


**Fig. 5.** The typical SEM images for the as-prepared samples. (a)–(c) are the general low magnification images, (d) and (e) are the medium magnification images, (f) is high magnification image.

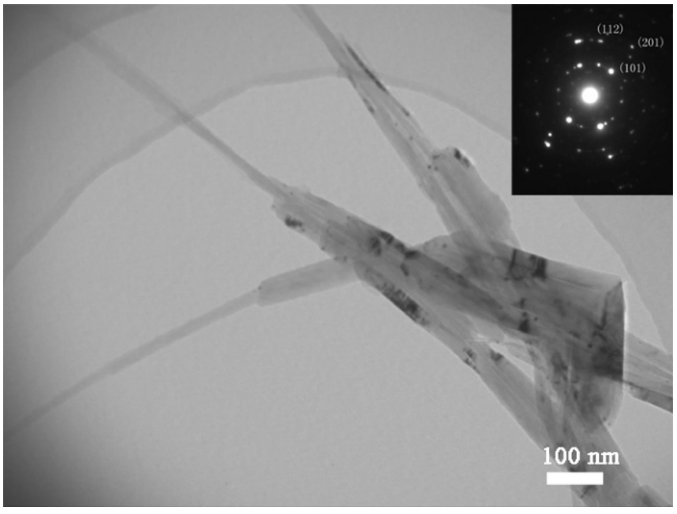


**Fig. 6.** The TEM and SAED images for the as-prepared samples.

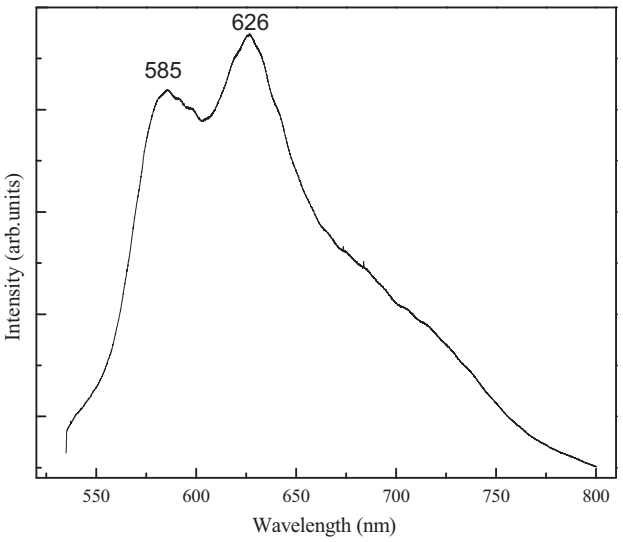


**Fig. 7.** The typical PL spectrum of the synthesized PtB nanowires.

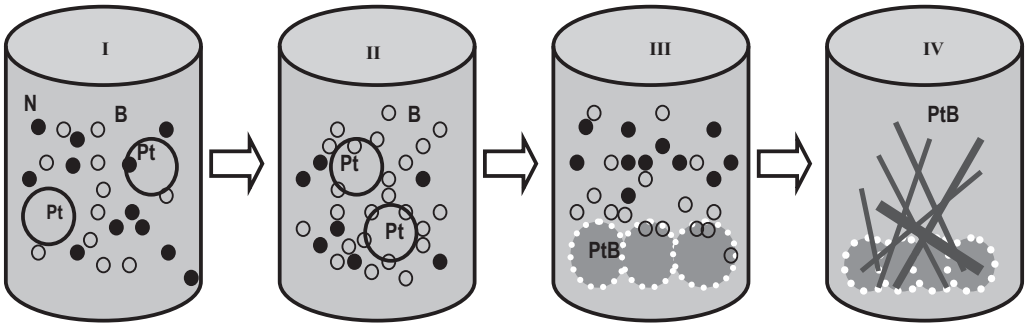


**Fig. 8.** Schematic of the growth processes of the PtB nanowires.

constant of Pt decreases slightly from 0.393 nm to 0.385 nm as the milling time increase.

Fig. 4 shows a typical XRD patterns of the sample prepared by the DC arc discharge technique, indicating that the sample consists of three phases, platinum boride (PtB), Pt and *a*-BN. That implies that some Pt react with B of *a*-BN to form PtB. The lattice constant of PtB calculated from the XRD data is $a = 3.343$ Å, $c = 4.062$ Å, respectively, in good agreement with the value given in the previous literature (JCPDS, No. 73-1846).

The low magnification SEM image of sample obtained by DC arc discharge reveals that the surface of product is composed of club-shaped structures about several tens of microns in size, as shown in Fig. 5(a). It is also found that the club-shaped structures wrap with the micron-scaled spherical droplets (Fig. 5(b)), we deduce it is caused by the VLS growth process for the sample. The micron-scaled architectures shown in Fig. 5(c) may result from the aggregation of the obtained PtB nanowires. However, from our XRD investigations it can be found that the final products contain another component Pt. The architectures are therefore composed of mixtures of PtB nanowires and Pt grains, rather than a pure PtB phase. Form the medium magnification SEM images of the sample (Fig. 5(d) and (e)), which present more details on the morphologies of these architectures, it can be seen that large quantities of PtB nanowires aggregate into bundle with the diameter of not more than 200 nm. Aggregation into linear shape morphologies seems to be a common phenomenon for nanostructures nucleated from liquid phases, for example, AlN nanostructures *via* controlled synthesis in CVD systems [22] and SiC nanowires in DC arc systems [23]. From the high magnification SEM images shown in Fig. 5(f), it can be observed that individual PtB nanowires of the sample are long and straight, randomly oriented, with clean and smooth surfaces. Typically, they are about 30–50 nm in stem diameter and 20–30 μm in length.

Furthermore, the morphology and structure of PtB nanowires have been characterized using TEM analysis. Fig. 6 shows TEM image of the typical PtB nanowires, 30–50 nm in diameter. It is clearly seen that the PtB nanowires were single crystalline, evidenced by the corresponding selected area electron diffraction (SAED) pattern as shown in the inset of Fig. 6.

A typical photoluminescence (PL) spectrum of the synthesized PtB nanowires is shown in Fig. 7. The excitation wavelength is 532 nm. Two broad PL emission peak can be clearly observed at about 585 nm and 626 nm. Since the PL spectra can reflect the optical effect of the material excited the lights with different wavelength, we can conclude that the as-prepared PtB nanowires might be regarded as the luminescence material though there is not any literature reported on the optical property.

The droplets at the tips of as-prepared PtB nanowires are found to be characteristic (Fig. 5 (b)), suggesting a vapor–liquid–solid (VLS) growth mechanism of the samples. We suggest the growing process of PtB nanowires as follow: As the DC arc is ignited, the tungsten rod (cathode) and the source materials (anode) in the graphite crucible are heated to $10^3$–$10^4$ °C. The solid mixtures of platinum and *a*-BN are evaporated drastically both thermally by the high temperature of the arc zone. The following reactions may proceed simultaneously.

$$a\text{-BN}(s) \rightarrow B(g) + N(g)$$

$$Pt(s) \rightarrow Pt(l) \rightarrow Pt(v)$$

$$Pt(v) + B(g) \rightarrow PtB(l) \rightarrow PtB(s)$$

Fig. 8 schematically illustrates the growth processes of the PtB nanowires. An underestimation of the temperature on the tip of the tungsten cathode to be no less than 2000 °C is reasonable. Pure platinum melts at 1772 °C. Therefore, the nanoparticles of platinum will melt and evaporated at such temperature, at the same time, boron atoms in the formed larger clusters enwrapped the platinum clusters prefer to migrate from the exterior surfaces to the centers, leading to the formation of PtB. As B atoms dissolved into the Pt liquid droplets, which upon supersaturating induced precipitation of solid PtB at the liquid–solid interface. As precipitation continues, the nanowires grow, with their diameters proportional in size to the Pt liquid droplets. As the reactive atoms and clusters depart from the central arc region, tiny liquid droplets come into being due to large temperature gradient. Once the tiny liquid droplets depart from the arc region and adhere to the water-cooled collecting wall, the species undergo a fast cooling process and aggregate into club-like structures.

It is worthy of noting that no platinum nitride (PtN) was observed in the as-prepared samples. Although both B and N atoms have the possibilities to react with platinum in the DC arc process, the existence of large formation-energy barriers of PtN made N atoms hardly react with Pt at low-pressure. Crowhurst et al. [24] have calculated the formation energies of zinc-blended structure PtN to be 183 kJ/mol, which is much higher than that of PtB (−10.4 kJ/mol) [25]. In fact, PtN have been synthesized successfully at above 45–50 GPa and temperatures exceeding 2000 K [24,26].

## 4. Conclusions

PtB nanowires have been prepared *via* the direct current arc discharge method using a milled mixture of platinum and boron nitride as precursor. XRD, TEM and SAED analyses confirm that the nanowire is composed of a single-crystalline PtB. A two-step growth process is proposed. First, the nucleation and formation of the Pt-rich droplets occur; Second, the nucleation and growth of the PtB nanowires proceed *via* a VLS mechanism with the Pt-rich droplets formed in the previous step. This synthesis of single-crystalline PtB nanowires opens the possibility of study of their physical and chemical properties.

## Acknowledgements

This work is supported by the Natural Science Foundation of China (No. 11074093), National Found for Fostering Talents of basic Science (No. J1103202), Natural Science Foundation of Jilin Province (No. 11074093), and the National Basic Research Program of China (Nos. 200903320 and 201103222).

## References

[1] Structure–Property Correlations for $TiB_2$-Based Ceramics Densified Using Active Liquid Metals, Science of Hard Materials, R.K. Viswanadham, D.J. Rowcliffe, J. Gurland (Eds.), Plenum Press, New York, 1983, p. 891.
[2] M.M. Opeka, I.G. Talmy, E.J. Wuchina, J.A. Zaykoski, S.J. Causey, J. Eur. Ceram. Soc. 19 (1999) 2405.
[3] W.G. Fahrenholtz, G.E. Hilmas, I.G. Talmy, J.A. Zaykoski, J. Am. Ceram. Soc. 90 (2007) 1347.
[4] D.B. Yigal, M. Jochen, H. David, A. Brian, V. Michael, J. Am. Ceram. Soc. 91 (2008) 1481.
[5] R.B. Kaner, J.J. Gilman, S.H. Tolbert, Science 308 (2005) 1268.
[6] H.Y. Chung, M.B. Weinberger, J.B. Levine, A. Kavner, J.M. Yang, S.H. Tolbert, R.B. Kaner, Science 316 (2007) 436.
[7] H.Y. Chung, M.B. Weinberger, J.M. Yang, S.H. Tolbert, R.B. Kaner, Appl. Phys. Lett. 92 (2008) 261904.
[8] A. Latini, J.V. Rau, R. Teghil, A. Generosi, V.R. Albertini, Appl. Mater. Interf. 2 (2010) 581.
[9] X.Q. Chen, C.L. Fu, M. Krcmar, G.S. Painter, Phys. Rev. Lett. 100 (2008) 196403.
[10] B. Aronsson, E. Stenberg, J. Aselius, Acta Chem. Scand. 14 (1960) 733.
[11] A.P. Alivisatos, Science 271 (1996) 933.
[12] E.W. Wong, P.E. Sheehan, C.M. Lieber, Science 277 (1997) 1971.
[13] X.Y. Tao, X.N. Wang, X.D. Li, Nano Lett. 7 (2007) 3172–3176.
[14] R. Li, L.H. Bao, X.D. Li, Cryst. Eng. Commun. 13 (2011) 5858–5862.
[15] L.H. Bao, Z.H. Xu, R. Li, X.D. Li, Nano Lett. 10 (2010) 255–262.
[16] H. Zhang, Q. Zhang, J. Tang, L.C. Qin, J. Am. Ceram. Soc. 127 (2005) 8002.
[17] T.T. Xu, J.G. Zheng, A.W. Nicholls, S. Stankovich, R.D. Piner, R.S. Ruoff, Nano Lett. 4 (2004) 2051.
[18] L. Lu, M.O. Lai, Mater. Design 16 (1995) 33.
[19] Z.H. Ding, B. Yao, L.X. Qiu, S.Z. Bai, X.Y. Guo, Y.F. Xue, W.R. Wang, X.D. Zhou, W.H. Su, J. Alloys Compds 391 (2005) 77.
[20] L.X. Qiu, B. Yao, Z.H. Ding, X.D. Zhao, H. Ji, X.B. Du, X.P. Jia, W.T. Zheng, Chin. Phys. Lett. 25 (2008) 1898.
[21] Z.H. Ding, L.X. Qiu, B. Yao, X.D. Zhao, F.G. Lu, X.Y. Liu, Chin. Phys. Lett. 27 (2010) 086106.
[22] H.T. Chen, X.L. Wu, X. Xiong, W.C. Zhang, L.L. Xu, J. Zhu, P.K. Chu, J. Phys. D: Appl. Phys. 41 (2008) 025101.
[23] J. Zhang, Q.S. Wang, F. Wang, X.H. Chen, W.W. Lei, Q.L. Cui, G.T. Zou, J. Phys. D: Appl. Phys. 42 (2009) 035108.
[24] J.C. Crowhurst, A.F. Goncharov, B. Sadigh, C.L. Evans, P.G. Morrall, J.L. Ferreira, A.J. Nelson, Science 311 (2006) 1275.
[25] A.N. Kolmogorov, S. Curtarolo, Phys. Rev. B 74 (2006) 224507.
[26] E. Gregoryanz, C. Sanloup, M. Somayazulu, J. Badro, G. Fiquet, H.K. Mao, R.J. Hemley, Nat. Mater. 3 (2004) 294.